Mass and isotopic yield distributions of fission-like events in the $^{19}F + ^{169}Tm$ system at low energies

Mohd. Shuaib,[1,*] Vijay R. Sharma,[2] Abhishek Yadav,[3] Swati Thakur,[4] Manoj Kumar Sharma,[5] Ishfaq Majeed,[1] Mahesh Kumar,[5] Pushpendra P. Singh,[4] Devendra P. Singh,[6] R. Kumar,[3] R. P. Singh,[3] S. Muralithar,[3] B. P. Singh,[1,†] and R. Prasad[1]

[1]*Nuclear Physics Laboratory, Physics Department, A. M. U, Aligarh 202 002, India*

[2]*Departamento de Aceleradores, Instituto Nacional de Investigaciones Nucleares, Apartado Postal 18-1027, C.P. 11801, Ciudad de Mexico, Mexico*

[3]*NP Group, Inter-University Accelerator Centre, New Delhi 110 067, India*

[4]*Department of Physics, Indian Institute of Technology, Ropar, Punjab 140 001, India*

[5]*Physics Department, S. V. College, Aligarh 202 001, India*

[6]*Department of Physics, University of Petroleum and Energy Studies, Dehradun 248 007, India*

(Received 21 August 2018; revised manuscript received 20 December 2018; published 21 February 2019)

In the present work, 22 fission-like residues with mass number $67 \leqslant A \leqslant 156$ produced via complete fusion-fission and/or incomplete fusion-fission have been identified and their production cross sections measured at three projectile energies, viz., 92.0 ± 1.8, 102.5 ± 1.5, and 105.4 ± 1.6 MeV in the $^{19}F + ^{169}Tm$ system. The absolute cross section of each fission-like residue is measured by recoil-catcher activation technique using off-line γ-ray spectroscopy. The data have been analyzed to deduce the parameters for isotopic yield and isobaric charge distributions. The deduced isotopic yields for indium (^{107,108,109,110m}In) and neodymium (^{134,135,137,139}Nd) isotopes are reproduced by Gaussian distribution and their variance is in good agreement with that reported in literature. The mass distributions of fission-like residues at three energies are also found to be Gaussian peaked, which confirms their production via deexcitation of a compound nucleus through complete fusion-fission and/or incomplete fusion-fission processes. It has been observed that, the mass variance (σ_M^2) values of fission fragments for two different systems, $^{12}C + ^{169}Tm$ and $^{19}F + ^{169}Tm$, at nearly the same excitation energy and angular momentum are distinctly different, indicating the importance of the entrance channel effect in fission reaction dynamics. The theoretically calculated isobaric charge dispersion parameters for these residues are found to be in good agreement with those obtained from the experimental data.

DOI: 10.1103/PhysRevC.99.024617

I. INTRODUCTION

The study of fission-like events associated with high spin matter produced in heavy ion (HI) interactions at moderate excitation energies has been a topic of interest for the last couple of decades [1,2]. In HI induced reactions, the formation of a heavy system takes place predominantly via two modes, viz., (i) complete fusion (CF) and (ii) incomplete fusion (ICF) processes [3–8]. The heavy composite system so formed may undergo fission [9–15] leading to the production of intermediate mass fragments. Further, at higher excitation energies, the nucleus is so excited that its shell properties can be neglected. Moreover, the system acquires a significant angular momentum (ℓ), which strongly affects the shape of the fissioning nucleus and lowers the fission barrier [16,17]. Attempts have been made to investigate the fusion-fission reactions at energies ≈5–7 MeV/nucleon [10,11,15]. Recent experimental data shows the presence of fission like events at energies ≈5-7 MeV/nucleon for the systems $^{12}C + ^{169}Tm$ [10],$^{16}O + ^{159}Tb$, ^{169}Tm [11], and $^{16}O + ^{181}Ta$ [15], where fusion is expected to be a dominant mode of reaction. Studies done by Sikkeland and Trautmann [18] indicate that the higher angular momentum (ℓ) may lead to the final state of fission via the ICF process. However, Viola *et al.* [19] studied the fission dynamics and estimated the critical angular momentum associated with the system, and correlated it without any major discrepancy with the rotating liquid drop model. They further indicated that fission becomes important with projectile energies above 10 MeV/nucleon. Nishio *et al.* [20] measured the angular distribution of fission fragments for the system $^{16}O + ^{238}U$, and from similar studies done on the systems $^{12}C + ^{233,235,238}U$ [21], $^{16}O + ^{232}Th$ [22], $^{16}O + ^{238}U$ [23], $^{19}F + ^{232}Th$ [24,25], and $^{40}Ar + ^{238}U$ [26] it may be concluded that fission following incomplete fusion dominates over fission following complete fusion in heavy ion reactions at intermediate energies. Hinde *et al.* [27] measured the angular distribution of fission fragments and the production cross section of the evaporation residues for the system $^{16}O + ^{238}U$ at energies ≈76–104 MeV. However, these measurements could not conclusively identify the path followed by the fissioning system: via fusion meadow or the fission valley [28]. Ghosh *et al.* [29] carried out precise measurements of mass distribution of fission fragments as a function of excitation energy, which can be used as a probe to determine the path

*shuaibphy67@gmail.com
†bpsinghamu@gmail.com

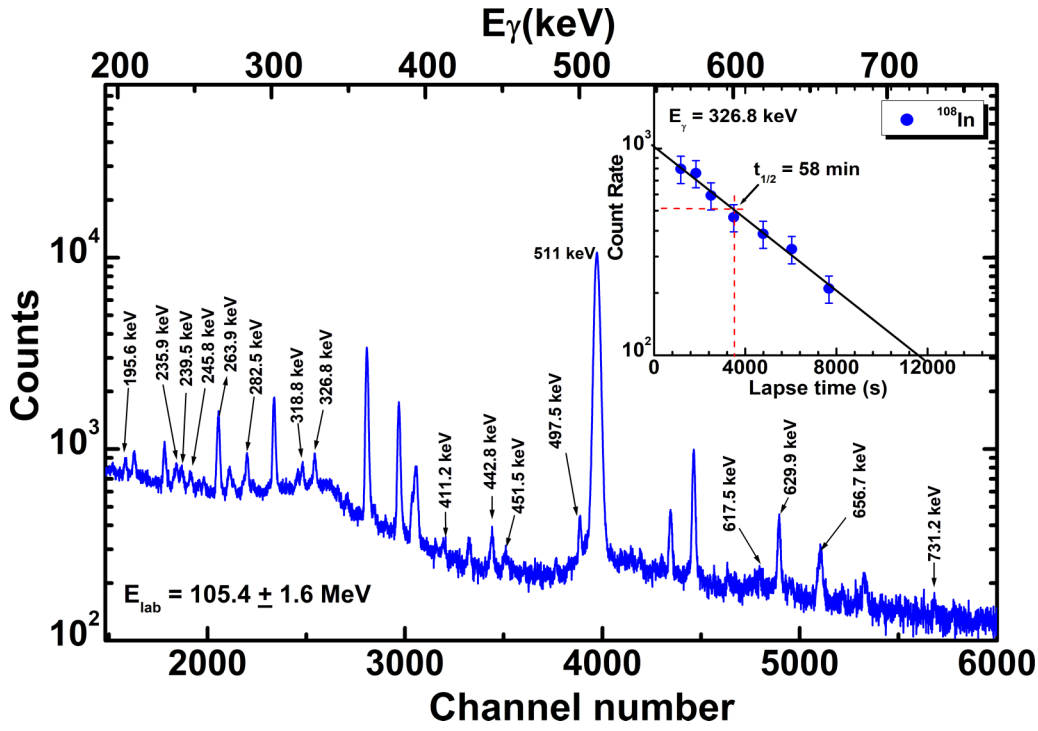

FIG. 1. A typical γ-ray spectrum of $^{19}\mathrm{F} + ^{169}\mathrm{Tm}$ interaction at 105.4 ± 1.6 MeV, where identified γ lines assigned to different reaction products expected to be populated via CFF and/or IFF processes are indicated.

followed by the systems. The measurements of variance in mass distributions of fission fragments from fusion-fission reactions on deformed targets exhibit a sharp anomalous increase with energy, in contrast to the smooth variation of variance for spherical targets [29]. It may be pertinent to mention that the charge and mass distributions are two essential post-fission observables that have been extensively studied at intermediate energies to understand the fading of shell effects in the dynamics of fission processes. Moreover, the cross-section data for fission-like events obtained from HI induced reactions are relevant to reactor technology, such as in accelerator-driven systems (ADS) for transmutation of nuclear waste and energy production [30]. Several attempts have been made to explain HI-induced fission for various entrance channel parameters, but a proper systematics for fission dynamics is still unclear and require a comprehensive investigation with more projectile and target combinations. In the present work, the production cross sections of residues likely to be populated through the fission of a compound nucleus (CN) formed via CF and/or ICF processes in the $^{19}\mathrm{F} + ^{169}\mathrm{Tm}$ system at three incident energies, viz., 92.0 ± 1.8, 102.5 ± 1.5, and 105.4 ± 1.6 MeV, have been measured. Analysis of data has been done to obtain the isotopic yield and the mass distributions of fission-like fragments. The mass variance (σ_M^2) of the fission-like residues has been deduced and its dependence on various entrance channel parameters has been studied.

The present paper is organized as follows: a brief description of the experimental methodology is given in Sec. II, while Sec. III deals with the details of analysis of data and their interpretation. Section IV represent the summary of the present work.

II. EXPERIMENTAL METHODOLOGY

Experiments to measure the production cross section of fission-like residues populated in the $^{19}\mathrm{F} + ^{169}\mathrm{Tm}$ system were carried out at the ion beam facility of the Inter-University Accelerator Centre (IUAC), New Delhi, India. The $^{19}\mathrm{F}^{+7}$ beam produced by the accelerator was focused on a $^{169}\mathrm{Tm}$ target. An activation technique followed by offline γ-ray spectroscopy was employed. The details of experimental methodology are given elsewhere [7]; however, for the sake of completeness, important details are summarized here. Isotopically pure (99.99%) $^{169}\mathrm{Tm}$ targets (thickness ≈1.0–1.5 mg/cm^2) and aluminum catcher/energy-degrader foils (thickness ≈1.5–2.5 mg/cm^2) were prepared by the rolling technique. To achieve the wide range of energy, an energy degradation technique was used in which each target foil is backed by an Al catcher foil (hereafter called the target-catcher assembly). In the present experiment, three stacks (each consisting of three target-catcher foil assemblies) were irradiated separately at 92.0, 102.5, and 105.4 MeV beam energies. The target at highest incident energy of each stack was used for analyzing the fission fragments. The irradiations were carried out in the General Purpose Scattering Chamber (GPSC) [31]. Considering the half-lives of interest, the irradiations were carried out for ≈8–10 h for each stack. The beam current was maintained ≈3–4 p nA throughout the irradiations and monitored using a Faraday cup installed downstream the beamline. The activities induced in the samples were recorded separately at several time intervals using a single high-purity germanium (HPGe) detector of 100 cm^3 active volume coupled to the computer-aided measurement and control (CAMAC) based data acquisition system CANDLE [32].

TABLE I. A list of identified fission fragments in the $^{19}F + ^{169}Tm$ system and their decay data.

Nuclides	E_γ (keV)	I_γ (%)	Half-life	Decay mode
^{67}Ge	912.3	3.1	18.9 min	I
^{75}Br	286.4	88	1.61 h	I
^{80}Sr	235.9	4.2	1.7 h	I
$^{84^m}$Rb	248.0	23.65	20.46 min	I
^{101}Mo	195.6	42.01	14.7 min	I
^{107}In	809.5	3.26	34.4 min	I
^{108}In	326.8	13.7	58 min	I
^{109}In	203.5	74	4.2 h	I
$^{110^m}$In	656.7	98	1.15 h	I
^{115}Sb	497.5	98	32 min	I
^{120}Xe	629.9	1.04	40 min	C
^{125}Cs	411.2	5.0	45.08 min	C
^{126}Ba	282.6	3.1	1.66 hr	I
^{128}Xe	442.8	7.0	40 min	I
^{130}Sb	731.2	22.0	39.5 min	I
^{131}Te	451.5	18.18	25 min	I
^{134}Nd	318.8	1.1	8.53 min	C
^{135}Nd	245.8	3.5	12.4 min	I
^{137}Nd	239.5	3.5	35.5 min	I
^{139}Nd	540.1	7.0	29.7 min	I
^{140}Sm	342.6	2.14	8.56 min	C
^{156}Ho	617.5	1.37	55.5 min	I

TABLE II. Measured cross sections of the fission products formed in the $^{19}F + ^{169}Tm$ system at three different energies.

Nuclides	92.0 MeV σ (mb)	102.5 MeV σ (mb)	105.4 MeV σ (mb)
^{67}Ge	3.4 ± 0.5	5.5 ± 0.8	8.9 ± 1.3
^{75}Br	7.5 ± 1.1	18.2 ± 2.7	23.1 ± 3.5
^{80}Sr	14.3 ± 2.1	29.1 ± 4.4	32.9 ± 4.9
$^{84^m}$Rb	4.1 ± 0.6	6.5 ± 0.9	8.7 ± 1.3
^{101}Mo	31.4 ± 4.7	36.8 ± 5.5	45.0 ± 6.7
^{107}In	19.8 ± 2.9	23.1 ± 3.5	25.6 ± 3.8
^{108}In	50.7 ± 7.6	55.3 ± 9.3	60.2 ± 9.0
^{109}In	45.7 ± 6.8	52.3 ± 9.8	55.1 ± 8.3
$^{110^m}$In	8.5 ± 1.3	10.1 ± 2.7	12.5 ± 1.8
^{115}Sb		30.6 ± 4.6	39.2 ± 5.8
^{120}Xe			47.8 ± 7.2
^{125}Cs	34.1 ± 5.1	39.2 ± 5.9	36.1 ± 5.4
^{126}Ba	55.7 ± 8.4	68.2 ± 10.2	73.3 ± 10.9
^{128}Xe	18.6 ± 2.8	19.4 ± 2.9	22.2 ± 3.3
^{130}Sb	34.5 ± 5.2	46.8 ± 7.0	55.3 ± 8.2
^{131}Te	22.1 ± 3.3	30.4 ± 4.5	37.7 ± 5.6
^{134}Nd	11.8 ± 1.8	18.3 ± 2.7	25.2 ± 3.7
^{135}Nd	17.2 ± 2.6	45.7 ± 6.8	49.4 ± 7.4
^{137}Nd	22.2 ± 3.3	68.1 ± 10.2	70.5 ± 10.5
^{139}Nd	12.6 ± 1.9	25.4 ± 3.8	29.1 ± 4.3
^{140}Sm	9.1 ± 1.4	16.1 ± 2.4	38.2 ± 5.7
^{156}Ho	1.1 ± 0.2	3.8 ± 0.5	5.2 ± 0.7

The resolution of the detector was 2 keV for the 1.33 MeV γ ray of a ^{60}Co source. The standard γ source and activity induced in the samples are recorded in the same geometry to avoid the errors introduced on account of the solid angle effect. The target-detector separation was adjusted so as to keep the dead time $<10\%$.

III. ANALYSIS OF DATA AND INTERPRETATION OF RESULTS

In order to measure the cross section of fission-like events populated via complete fusion-fission (CFF) and incomplete fusion-fission (IFF) at each studied energy, the residues have been identified from the recorded γ spectra by identifying their characteristic γ-ray energies and further confirmed by the decay curve analysis. Here, each sample was counted many times to obtain the half-lives of the residues. As a representative case, a typical γ-ray spectrum of the $^{19}F + ^{169}Tm$ system at energy 105.4 MeV is shown in Fig. 1. Further, as a typical example, the decay curve of ^{108}In ($t_{1/2} = 58$ min) residues obtained by following the 326.8 keV γ line is also shown in the inset of Fig. 1, and is in good agreement with the literature value and confirms its identification. The nuclear data such as half-life, γ-ray energies, intensities, etc., of the identified reaction residues have been taken from the *Table of Radioactive Isotopes* [33] and are listed in Table I.

After the identification of fission-like residues, the production cross section (σ_r) was determined by using the standard formulation [8]. The uncertainties in the measured cross sections may arise due to several factors [34]. The overall error, including the statistical errors is estimated to be $\leqslant 15\%$. The production cross section of ERs expected to be populated via CF and/or ICF processes in the $^{19}F + ^{169}Tm$ system have been measured in a separate experiment [7] and analyzed within the framework of statistical model code PACE4 [35]. Analysis of data indicates that measured EFs of *xn* and *pxn* channels are well reproduced by the statistical model calculations for level density parameter $a = A/10$ MeV^{-1} and confirms the production of these channels via CF mode. However, a significant enhancement in the production cross section of α-emitting channels has been observed and clearly manifests that enhancement may be attributed to the prompt breakup of the projectile at the studied range of energies [7]. Employing the same procedure, the production cross sections of fission-like residues populated via CFF and IFF processes have also been measured.

A. Measurement of production cross-sections of fission-like events and their distributions

In the present work, 22 fission-like residues in the range $67 \leqslant A \leqslant 156$ have been identified and are listed in Table I, along with their spectroscopic properties. Here, 18 fission-like residues are expected to have independent yields as they do not have feeding from a pre-cursor, and they are marked as I; whereas 4 fission-like residues are found to have cumulative yields as they are fed by a precursor, and they are marked as C. The production cross sections of fission-like residues were measured at three energies, employing the standard formulation [8], and they are given in Table II.

It may be pointed out that in the analysis of data the isotopes of indium (^{107,108,109,110m}In) and neodymium (^{134,135,137,139}Nd) were identified, and their isotopic yield distributions are presented in the following subsection.

B. Isotopic yield distributions of indium and neodymium isotopes

In a heavy composite system, at moderate excitation energies, the emission of particles (charged and/or uncharged) competes with fission. In such reactions, emanation of charged particles is sorely inhibited due to the large Coulomb barrier. Therefore, the emission of particles from the fission fragments may give rise to the isotopic and isobaric distributions of the fission residues. As already mentioned, neutron emission is more probable compared to proton emission, and therefore in most cases only isotopic yield distribution is experimentally observed. As a result, the study of isotopic distribution is one of the most fundamental approaches for modeling low energy fission. Further, it has been established that the independent isotopic yields are well expressed by a Gaussian distribution [36]. In the present work, four isotopes of indium (^{107,108,109,110m}In) and neodymium (^{135,136,137,139}Nd) have been identified at 92.0, 102.5, and 105.4 MeV beam energies, and their measured production cross sections have been fitted with Gaussian distribution given by

$$Y(A') = \sum_{1}^{n} P_n \frac{Y_Z}{\sqrt{2\pi\sigma_{A'}^2}} e^{-(A'-A'_P)^2/2\sigma_{A'}^2} \quad (1)$$

where $Y(A')$ is the independent yield of identified isotopes and Y_Z is the chain yield of isotopes. The dispersion parameters A'_P and $\sigma_{A'}^2$ are the most probable mass and variance obtained from the Gaussian distribution that followed the isotopic yield distribution. Figures 2(a)–2(c) and 3(a)–3(c) represent the isotopic yield distributions of indium and neodymium isotopes respectively at three energies. It may be pertinent to mention that the value of chi squared (χ^2) has been minimized by a nonlinear least-squares fit routine using ORIGIN software. As a representative case, for indium isotopes, the values of A'_P and $\sigma_{A'}^2$ at energy 105.4 MeV are found to be 108.37 and 4.97 ± 1.30, which is quite consistent with the values 108.42 and 4.16 ± 0.01 reported at energy 100 MeV for the ^{16}O + ^{181}Ta [15] system and 107.88 and 4.24 at energy 95 MeV for the ^{16}O + ^{169}Tm [11] system. The variance (σ_A^2) of the isotopic yield distribution obtained from the Gaussian fit for the two isotopes (In and Nd) at three excitation energies are compared with those reported in literature and are listed in Table III. It is apparent from Table III that the variance (σ_A^2) values deduced in the present work are in good agreement with the reported values for similar systems.

As demonstrated by Gubbi *et al.* [37], to deduce the total yield of a nuclide with mass number A, it is necessary to have the information of the isobaric charge dispersion parameter (σ_Z) and the most probable charge (Z_P), which has the highest yield among all the products of given mass. As such, these studies also provide access to the distribution of nuclear charge between the two complementary fission fragments for a given nucleus that undergoes fission. The fractional

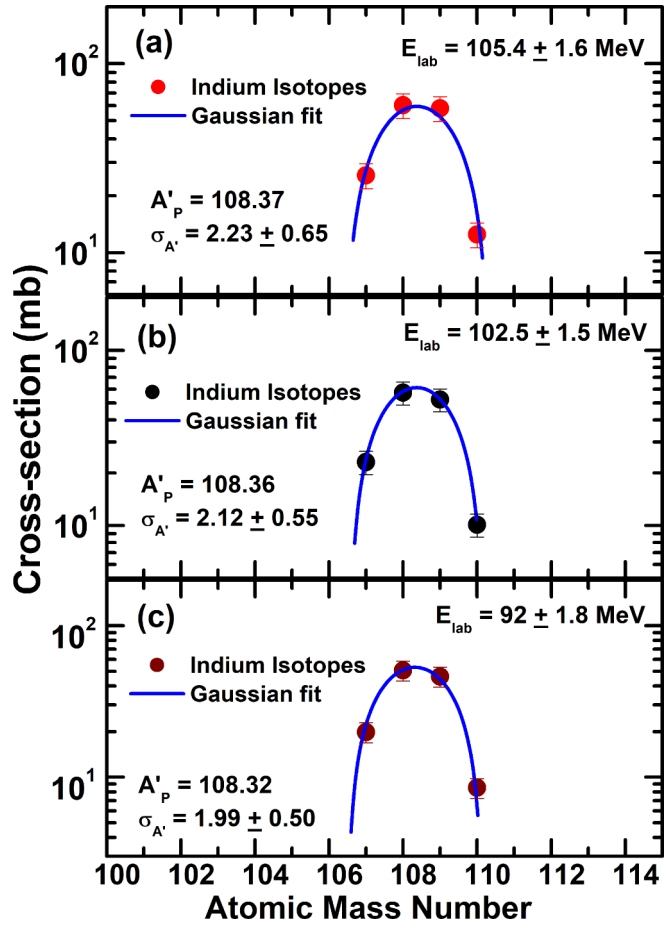

FIG. 2. Isotopic yield distribution of indium isotopes (^{107,108,109,110m}In) measured at three incident energies. The blue line is the Gaussian fit (see text for details).

independent isotopic yield (FY') for indium and neodymium isotopes is obtained by dividing the independent yield by the corresponding charge yield. The most probable charge (Z_P) for In and Nd isotopes is calculated using the relation

$$Z_P(A) = \frac{Z}{A_P} A, \quad (2)$$

where Z and A are the atomic number and the atomic mass number of the fission fragments respectively. The experimentally determined yields of In and Nd were normalized to obtain their respective fractional independent yield (FY') and are presented in Figs. 4(a)–4(c) and 5(a)–5(c), as a function of $Z - Z_P$. Using the Gaussian fitting procedure, the values of isobaric charge dispersion parameter (σ_Z) for In and Nd isotopes are obtained and tabulated in Table IV. As a representative case, the estimated values of σ_Z from the Gaussian fitting at excitation energies 71.2, 69.4, and 58.5 MeV for indium isotopes are found to be 0.94 ± 0.04, 0.89 ± 0.09, and 0.83 ± 0.02 charge units. Further, the values of σ_Z were calculated by converting the width parameter of isotopic yield (σ_A) to σ_Z by using the relation discussed in Ref. [37],

$$\sigma_Z = \frac{\sigma_A}{A_P} Z. \quad (3)$$

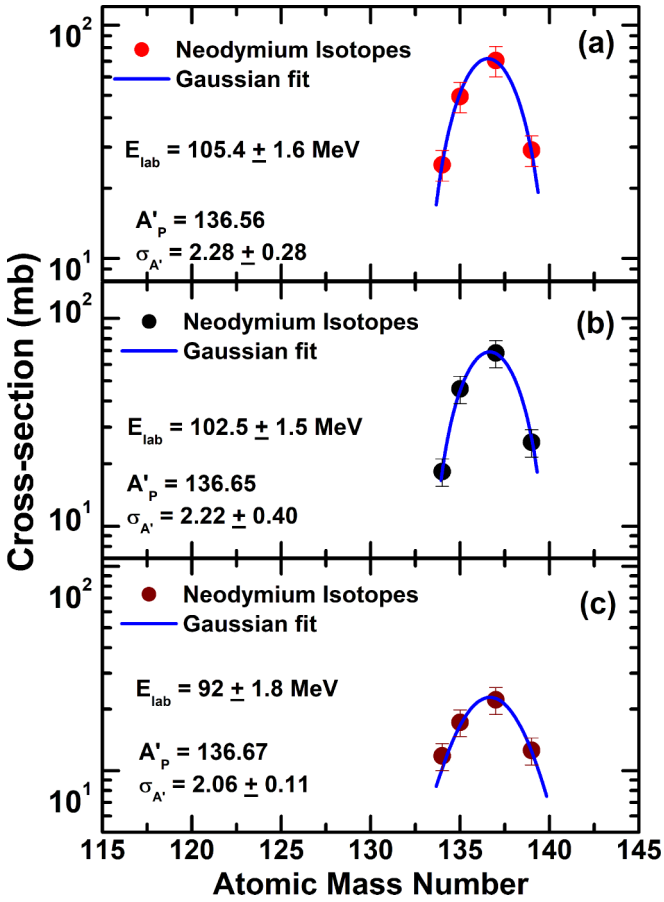

FIG. 3. Isotopic yield distribution of neodymium isotopes (^{134,135,137,139}Nd) measured at three incident energies. The blue line is the Gaussian fit (see text for details).

The value of σ_Z calculated using Eq. (3) for In and Nd isotopes and estimated isobaric charge distributions from Figs. 4 and 5 are also given in Table IV. As can be seen from this Table, the σ_Z values obtained from Eq. (3) are reasonably in agreement with those estimated from fitting of charge distribution. The above method indicates the self-consistency of the present work.

C. Mass distribution of fission like events

The mass distribution of fission fragments is one of the important post fission observables that is directly related to the collective dynamics of the fission process [38,39]. As already mentioned, the activities produced in the target-catcher foils were used to determine the fission mass distribution. The experimentally measured production cross sections of fission fragments expected to be populated via CFF and/or IFF processes in the ^{19}F + ^{169}Tm system at three incident laboratory energies, viz., 105.4, 102.5, and 92.0 MeV, are shown in Figs. 6(a)–6(c). In the present work, the mass distribution of fission fragments is found to be symmetric. This may be due to the fact that, generally, the compound nucleus forms with an excitation energy that is larger than the fission barrier. The centroid and width, which represent the most probable mass and dispersion parameter (σ_M) of fission fragments estimated from the fitting of Gaussian function, are found to be 107.8 ± 0.4 and 20.81 ± 0.75 at $E_{\rm lab} = 105.4$ MeV; 109.2 ± 0.3 and 18.96 ± 0.22 at $E_{\rm lab} = 102.5$ MeV; and 110.7 ± 0.2 and 15.56 ± 0.61 at $E_{\rm lab} = 92$ MeV.

The behavior of the saddle point and its stability for any system against the mass asymmetry (α) is given by the quantity called the Businaro-Gallone point (α_{BG}) [40], which is defined as the mass asymmetry for which the potential energy (saddle point) is maximum for a given fissility ($x = Z^2/A$), and is given by Eq. (4). The α_{BG} point can be used to explore the behavior of the saddle point and its stability against mass asymmetry. This is important in the sense that the direction

TABLE III. Comparison of variance (σ_A^2) of isotopic yield distribution for different fissioning systems.

System	E^* (MeV)	Isotope	σ_A^2	Ref.
^{19}F + ^{169}Tm	71.2	Nd	5.19 ± 0.56	[a]
^{19}F + ^{169}Tm	71.2	In	4.97 ± 1.30	[a]
^{19}F + ^{169}Tm	69.4	Nd	4.92 ± 0.80	[a]
^{19}F + ^{169}Tm	69.4	In	4.49 ± 1.10	[a]
^{19}F + ^{169}Tm	58.5	Nd	4.24 ± 0.22	[a]
^{19}F + ^{169}Tm	58.5	In	3.96 ± 1.0	[a]
^{16}O + ^{181}Ta	67.04	In	4.16 ± 0.01	[15]
^{16}O + ^{181}Ta	67.04	Y	3.05 ± 0.10	[15]
^{16}O + ^{169}Tm	61.06	In	4.24	[11]
^{16}O + ^{169}Tm	61.06	Tc	4.62	[11]
^{12}C + ^{169}Tm	68.6	Kr	3.90 ± 0.20	[10]
^{12}C + ^{169}Tm	68.6	Tc	3.27 ± 0.18	[10]
^{12}C + ^{169}Tm	62.9	Kr	3.05 ± 0.18	[10]
^{12}C + ^{169}Tm	62.9	Tc	2.94 ± 0.28	[10]
^{16}O + ^{159}Tb	57.1	Sr	3.31	[11]
^{16}O + ^{159}Tb	57.1	Y	4.41	[11]
^{7}Li + ^{232}Th	41.7	Sb	4.08	[44]
^{7}Li + ^{232}Th	41.7	I	3.96	[44]
^{11}B + ^{232}Th	55.7	Sb	4.0	[26]
^{11}B + ^{232}Th	55.7	I	5.43	[26]
^{11}B + ^{232}Th	55.7	Cs	3.72	[26]
^{11}B + ^{238}U	67.4	Rb	3.84 ± 0.16	[45]
^{11}B + ^{238}U	67.4	Cs	3.95 ± 0.14	[45]
^{22}Ne + ^{238}U	64.5	Rb	4.23 ± 0.40	[45]
^{22}Ne + ^{238}U	64.5	Cs	4.26 ± 0.90	[45]
^{22}Ne + ^{208}Pb	46.4	Sb	3.43 ± 1.02	[46]
^{22}Ne + ^{208}Pb	46.4	I	3.95 ± 0.87	[46]

[a]Present work.

TABLE IV. The isobaric charge dispersion parameter obtained from the Gaussian fit (see Fig. 6) and using Eq. (3).

E^* (MeV)	Isotope	σ_Z from Figs. 4 and 5	σ_Z from Eq. (3)
71.2	Nd	0.90 ± 0.03	1.0
71.2	In	0.94 ± 0.04	1.0
69.4	Nd	0.90 ± 0.03	1.0
69.4	In	0.89 ± 0.09	1.0
58.5	Nd	0.88 ± 0.02	0.9
58.5	In	0.83 ± 0.02	0.9

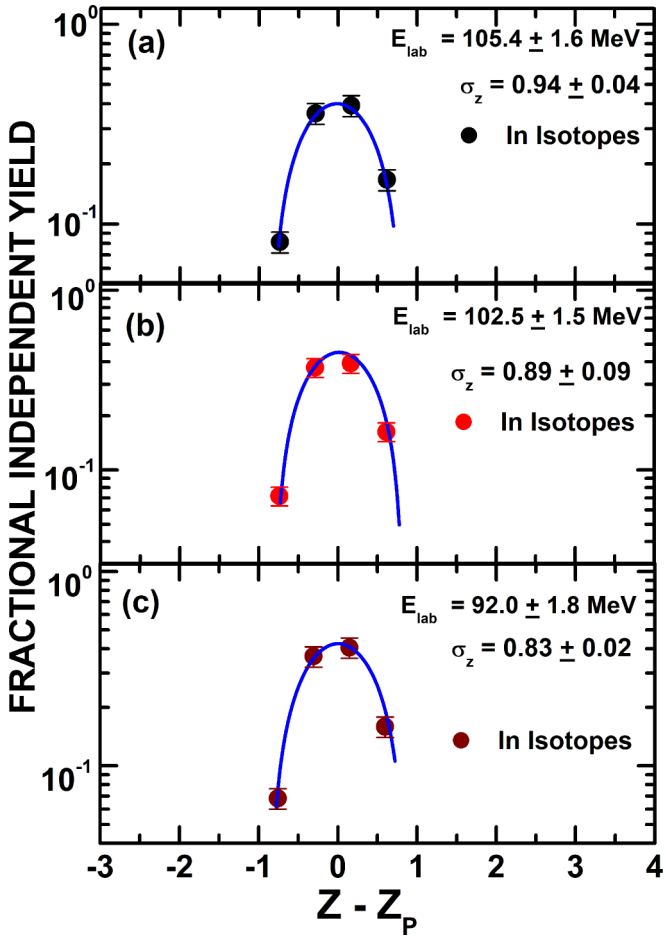

FIG. 4. Fractional independent yield (FY') distribution for indium isotopes (^{107,108,109,110m}In) corresponding to corrected charge distribution. The blue line is the Gaussian fit (see text for details).

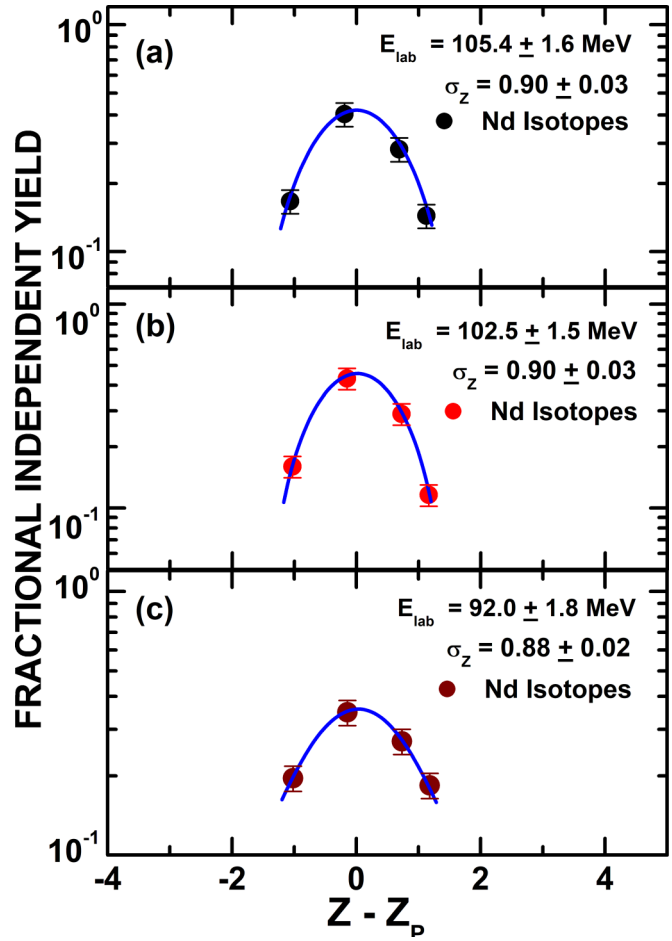

FIG. 5. Fractional independent yield (FY') distribution for neodymium isotopes (^{134,135,137,139}Nd) corresponding to corrected charge distribution. The blue line is the Gaussian fit (see text for details).

of mass drift between the two sides of a dinuclear system is expected to be decided by the potential energy landscape, and the value of α_{BG} determines whether the dinuclear system at contact will move dynamically towards higher mass asymmetry or mass symmetry. It has been observed that, if the mass asymmetry $\alpha = (M_T - M_P/(M_P + M_T)$ is larger than the Businaro-Gallone critical mass asymmetry α_{BG}, the system favors the mass drift towards higher mass-asymmetries. On the other hand, if $\alpha < \alpha_{BG}$, then the system favors mass drift towards more symmetric di-nuclear systems, resulting into a compact mononuclear shape equilibrating to a CN, and may overcome a mass-asymmetric saddle shape leading to quasifission. It has been demonstrated that the following expression [40] gives good estimates for the values of α_{BG}:

$$\alpha_{BG} = P\sqrt{\frac{(x - x_{BG})}{x - x_{BG} + q}}, \tag{4}$$

where $P = 1.12$ and $q = 0.24$ are the empirical constants, x is the fissility parameter, which is the ratio of Coulomb energy to the surface energy, and $x_{BG} = 0.396$ ($\approx$0.4). The critical mass asymmetry (α_{BG}) for the present system is found to be 0.82, whereas, the mass asymmetry (α) for the presently studied system is 0.79, which is less than the critical mass asymmetry ($\alpha_{BG} \approx 0.82$). This clearly indicates a broader and symmetric distribution of fission-like events, as expected from the Businaro-Gallone mass asymmetry formalism [40]. The values of mass variance (σ_M^2) of fission fragments are found to be 433.1 ± 34.6 at $E_{\rm Lab} = 105.4$ MeV, 359.5 ± 28.7 at $E_{\rm Lab} = 102.5$ MeV, and 242.1 ± 19.3 at $E_{\rm Lab} = 92.0$ MeV. The uncertainties quoted in these values are the fitting errors. To understand how the mass variance (σ_M^2) of fission fragments varies with excitation energy, the estimated σ_M^2 of fission fragments at three excitation energies ($E^* = 71.2$, 69.4, and 58.5 MeV) are plotted in Fig. 7. As can be seen from this figure, the σ_M^2 increases as the excitation energy of the system increases, indicating larger spread in the distribution of fission fragment masses at higher excitation energies, and follows the increasing trend as reported by Ghosh *et al.* [29] for ^{19}F, ^{16}O, and ^{12}C projectiles on ^{232}Th target.

For better insight into the fission dynamics and to understand the role of entrance channel parameters on mass distributions of fission fragments, the mass variance of fission-like products for different projectile-target combinations as a function of mass-asymmetry is shown in Fig. 8. It is clearly

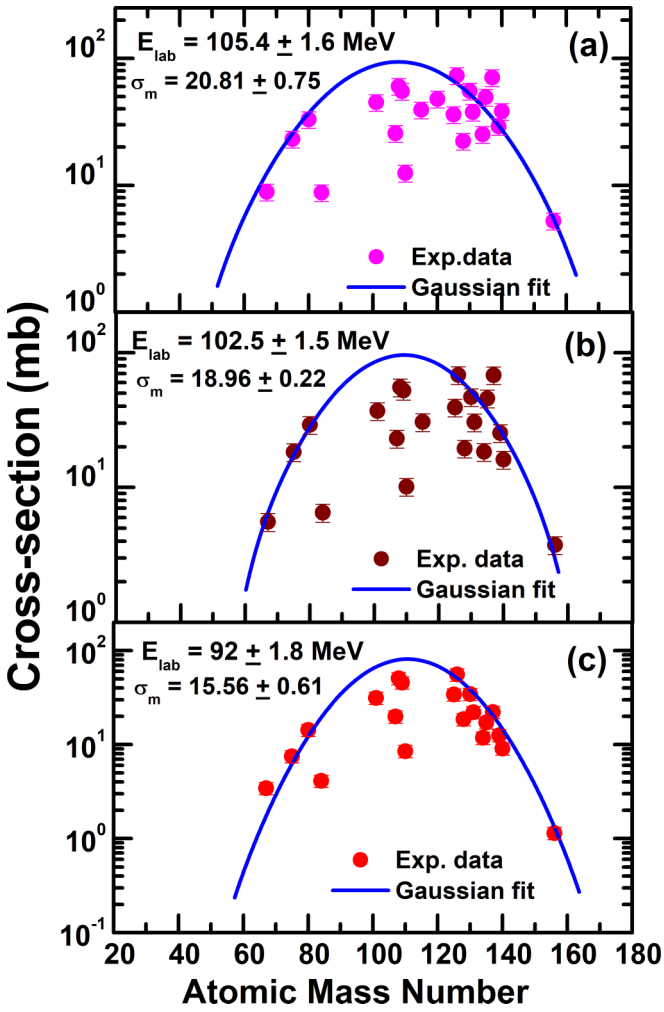

FIG. 6. Mass distribution of fission-like events populated via complete fusion-fission and/or incomplete fusion-fission processes in the $^{19}\mathrm{F} + {}^{169}\mathrm{Tm}$ system at studied energies. The solid blue line is the Gaussian fitting (see text for details).

apparent from this figure that the mass variance of fission-like residues for three projectile-target combinations, viz., $^{19}\mathrm{F} + {}^{169}\mathrm{Tm}$ (present work), $^{19}\mathrm{F} + {}^{209}\mathrm{Bi}$ [41], and $^{16}\mathrm{O} + {}^{232}\mathrm{Th}$ [42], at constant normalized energy ($E/V_b = 1.12$) follows a linear systematic rise with the increase in mass asymmetry of the system. Similar observations have been made by Karamyan *et al.* [43].

As discussed earlier, in the rotating liquid drop model (RLDM) and other theoretical representations, the fission barrier is strongly influenced by the angular momentum associated with the system, and it decreases as the value of angular momentum of the system increases. In the present work, a strong dependance of mass variance (σ_M^2) of fission-like fragments on excitation energy (E^*) and mass asymmetry (α) has been observed. As a result, an attempt has been made to understand the role of entrance channel parameters on fission dynamics. Figure 9 represents the variation of grazing angular momentum (ℓ_{graz}) with the excitation energy (E^*) for two systems, viz., $^{12}\mathrm{C} + {}^{169}\mathrm{Tm}$ [10] and $^{19}\mathrm{F} + {}^{169}\mathrm{Tm}$ (present work). The values of grazing angular momentum at different

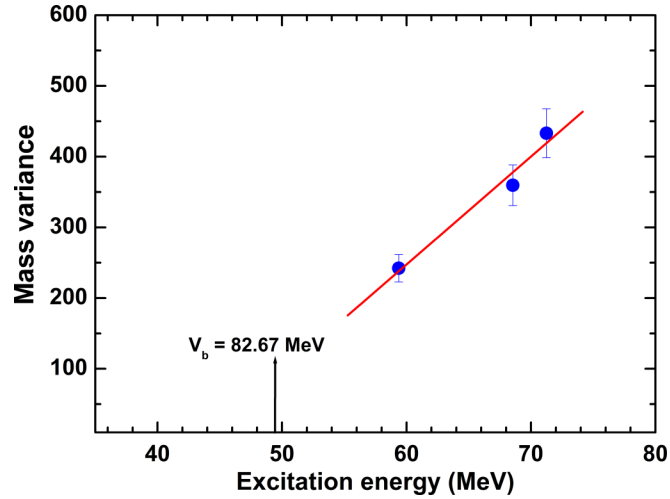

FIG. 7. The observed mass variance (σ_M^2) of fission fragment distribution plotted as a function of excitation energy (E^*) for the $^{19}\mathrm{F} + {}^{169}\mathrm{Tm}$ system. The solid line shows the linear increase in σ_M^2 with E^*. The vertical arrow indicates the value of excitation energy corresponding to the Coulomb barrier of the system.

excitation energies have been calculated using the PACE4 code [35]. As can be seen from this figure, there is a crossing point for the two curves at nearly same E^* (≈69 MeV) and ℓ_{graz} (≈42$\hbar$). The value σ_M^2 obtained from the mass distribution of fission fragments for $^{19}\mathrm{F} + {}^{169}\mathrm{Tm}$ (present work) system at $E^* \approx 69$ MeV is found to be 359.5 ± 28.7, which is entirely different from the variance ($\sigma_M^2 = 434 \pm 26$) reported for the system $^{12}\mathrm{C} + {}^{169}\mathrm{Tm}$ [10] at the same excitation energy. The difference in the values of mass variance (σ_M^2) for the two systems at nearly the same excitation energy and angular momentum may be attributed to the entrance channel effect. To clarify the above aspect, more experimental data are required, which may be useful to develop the systematics for fission dynamics.

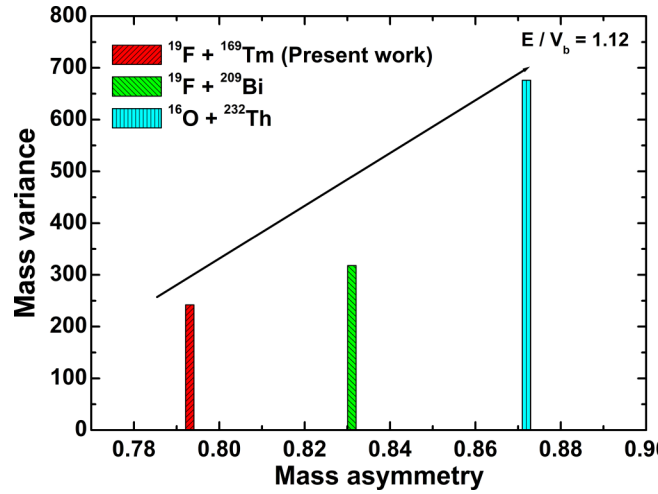

FIG. 8. A comparison of mass variance (σ_M^2) with mass asymmetry at constant normalized energy ($E/V_b = 1.12$) for three different systems, viz., $^{19}\mathrm{F} + {}^{169}\mathrm{Tm}$ (present work), $^{19}\mathrm{F} + {}^{209}\mathrm{Bi}$ [41], and $^{16}\mathrm{O} + {}^{232}\mathrm{Th}$ [42] (see text for details).

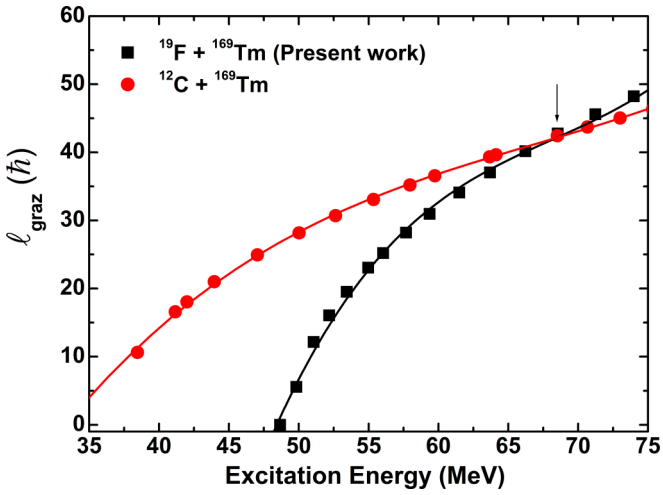

FIG. 9. A plot of grazing angular momentum (ℓ_{graz}) imparted to the system as a function of excitation energy (E^*) for the same deformed nucleus ^{169}Tm for two different projectiles, ^{12}C and ^{19}F. At the crossing point indicated by arrow, the two systems have nearly the same excitation energy and grazing angular momentum.

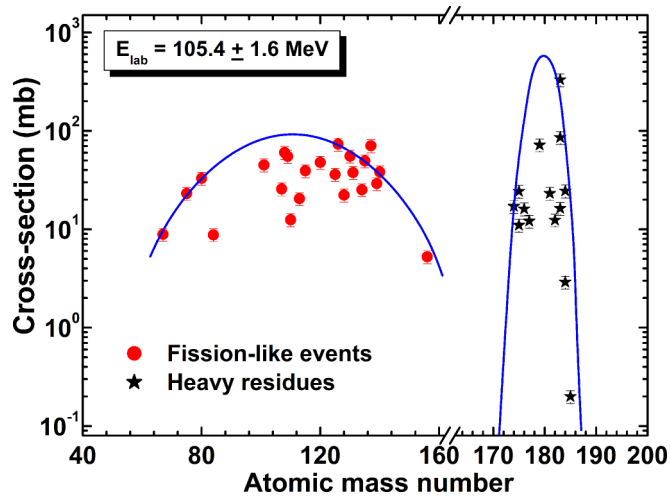

FIG. 10. Mass distribution of identified fission fragments and heavy residues populated via complete fusion and/or incomplete fusion processes at $E_{lab} = 105.4$ MeV. The solid lines are the Gaussian fitting (see text for details).

Figure 10 represents the production cross section of all identified residues (CF, ICF, and fission fragments) formed in the interaction of the $^{19}\mathrm{F} + {}^{169}\mathrm{Tm}$ system. In HI-induced reactions, the observed masses of residues may have three components, due to (i) CF and/or ICF residues, (ii) fission-like residues, and (iii) few-nucleon transfer residues or projectile-like fragments (PLFs). As can be observed from Fig. 10, in the lower mass region, the PLFs could not be detected due to their relatively higher energy and very short half-lives. However, for intermediate range masses, the mass distribution is found to be broad and symmetric, whereas the narrow peak at higher masses indicates the formation of these residues via CF and/or ICF events.

IV. SUMMARY AND CONCLUSIONS

In the present work, the production cross sections of a large number of fission-like residues $67 \leqslant A \leqslant 156$ populated via CFF and/or IFF in the $^{19}\mathrm{F} + {}^{169}\mathrm{Tm}$ system have been measured. The dispersion parameters to study the isotopic yield and isobaric charge distributions of two fission-like residues (indium and neodymium) have been obtained. The estimated isotopic yield distributions of In and Nd isotopes are found to be in reasonably good agreement with that reported in literature. The mass distributions of fission fragments at three incident energies are found to be symmetric, and they manifest the population of fission-like fragments via deexcitation of the compound nucleus. The dependence of mass variance on the entrance channel parameters, viz., excitation energy, mass-asymmetry, and grazing angular momentum, are studied. At constant normalized energy ($E/V_b = 1.12$), systematic linear growth in mass variance is observed as the mass asymmetry of the systems increases, indicating a broader distribution of fission fragments. The mass variance of fission fragments is found to be more for higher excitation energies. Further, at nearly the same excitation energy and angular momentum for the two systems $^{19}\mathrm{F} + {}^{169}\mathrm{Tm}$ (present work) and $^{12}\mathrm{C} + {}^{169}\mathrm{Tm}$ [10], the values of mass variance of fission fragments are found to be distinctly different, which is attributed to the entrance channel effects. To get a conclusive picture of the above facts, experiments involving direct mass-distribution measurements employing multiwire proportional counters along with neutron detectors are proposed.

ACKNOWLEDGMENTS

The authors thank to the Director of IUAC, New Delhi and the Chairperson, Department of Physics, A. M. U, Aligarh for providing all the necessary facilities to carry out this work. M.S. and B.P.S. thank the DST-SERB for financial support under Project No. EMR/2016/002254.

[1] J. B. Wilhelmy, M. Begemann-Blaich, T. Blaich, J. Boissevain, M. M. Fowler, A. Gavron, B. V. Jacak, P. S. Lysaght, H. C. Britt, D. J. Fields *et al.*, Nucl. Phys. A **502**, 601c (1989).

[2] S. E. Vigdor, H. J. Karwowski, W. W. Jacobs, S. Kailas, P. P. Singh, F. Soga, and T. G. Throwe, Phys. Rev. C **26**, 1035 (1982).

[3] A. Diaz-Torres and I. J. Thompson, Phys. Rev. C **65**, 024606 (2002); Phys. Rev. Lett. **98**, 152701 (2007).

[4] E. Z. Buthelezi, E. Gadioli, G. F. Steyn, F. Albertini, C. Birattari, F. Cerutti, S. H. Connell, A. A. Cowley, E. Fabrici, and E. Gadioli Erba, Nucl. Phys. A **734**, 553 (2004).

[5] P. R. S. Gomes, I. Padron, E. Crema, O. A. Capurro, J. O. Fernández Niello, A. Arazi, G. V. Martí, J. Lubian, M. Trotta, A. J. Pacheco *et al.*, Phys. Rev. C **73**, 064606 (2006); P. R. S. Gomes, I. Padron, M. D. Rodríguez, G. V. Martí, R. M. Anjos,

J. Lubian, R. Veiga, R. Liguori Neto, E. Crema, N. Added *et al.*, Phys. Lett. B **601**, 20 (2004).
[6] M. Dasgupta, D. J. Hinde, A. Mukherjee, and J. O. Newton, Nucl. Phys. A **787**, 144 (2007).
[7] M. Shuaib, V. R. Sharma, A. Yadav, P. P. Singh, M. K. Sharma, D. P. Singh, R. Kumar, R. P. Singh, S. Muralithar, B. P. Singh, and R. Prasad, J. Phys. G: Nucl. Part. Phys. **44**, 105108 (2017) and references therein.
[8] R. Prasad and B. P. Singh, *Fundamentals and Applications of Heavy Ion Collisions* (Cambridge University Press, Cambridge, 2018).
[9] L. G. Moretto *et al.*, in International Atomic Energy Agency Symposium on Fission, Rochester, New York, 1973, Paper No. SM174/75 (unpublished).
[10] A. Sood, P. P. Singh, R. N. Sahoo, P. Kumar, A. Yadav, V. R. Sharma, M. Shuaib, M. K. Sharma, D. P. Singh, and U. Gupta, Phys. Rev. C **96**, 014620 (2017).
[11] P. P. Singh, B. P. Singh, B. Sharma, Unnati, M. K. Sharma, and R. Prasad, Int. J. Mod. Phys. E **17**, 549 (2008).
[12] W. Udo Schroder, Pramana J. Phys. **85**, 227 (2015).
[13] D. J. Hinde, M. Dasgupta, M. Evers, C. J. Lin, D. H. Luong, R. du Rietz, C. Simenel, A. Wakhle, and E. Williams, J. Phys.: Conf. Ser. **420**, 012115 (2013).
[14] W. Gawlikowicz, D. K. Agnihotri, S. A. Baldwin, W. U. Schroder, J. Tõke, R. J. Charity, D. G. Sarantites, L. G. Sobotka, R. T. deSouza, T. Barczyk *et al.*, Phys. Rev. C **81**, 014604 (2010).
[15] V. R. Sharma, A. Yadav, P. P. Singh, M. K. Sharma, D. P. Singh, Unnati, R. Kumar, K. S. Golda, B. P. Singh, A. K. Sinha *et al.*, Phys. Rev. C **84**, 014612 (2011).
[16] A. J. Sierk, Phys. Rev. C **33**, 2039 (1986).
[17] S. Cohen, F. Plasil, and W. J. Swiatecki, Ann. Phys. (N.Y.) **82**, 557 (1974).
[18] T. Sikkeland, E. L. Haines, and V. E. Viola, Jr., Phys. Rev. **125**, 1350 (1962).
[19] V. E. Viola, K. Kwiatkowski, and M. Walker, Phys. Rev. C **31**, 1550 (1985).
[20] K. Nishio, H. Ikezoe, Y. Nagame, M. Asai, K. Tsukada, S. Mitsuoka, K. Tsuruta, K. Satou, C. J. Lin, and T. Ohsawa, Phys. Rev. Lett. **93**, 162701 (2004).
[21] M. C. Duh, H. Baba, N. Takashi, A. Yokoyama, T. Saito, S. Baba, and K. Hata, Nucl. Phys. A **550**, 281 (1992).
[22] J. P. Lestone, J. R. Leigh, J. O. Newton, and J. X. Wei, Nucl. Phys. A **509**, 178 (1990).
[23] A. Pagano, S. Aiello, E. DeFilippo, G. Lanzanó, S. Lo Nigro, C. Milone, G. Blancato, G. DiMarco, and M. C. Mermaz, Phys. Rev. C **47**, 1170 (1993).
[24] D. J. Hinde, J. R. Leigh, J. J. M. Bokhorst, J. O. Newton, R. L. Walsh, and J. Boldeman, Nucl. Phys. A **472**, 318 (1987).
[25] G. K. Gubbi, A. Goswami, B. S. Tomar, B. John, A. Ramaswami, A. V. R. Reddy, P. P. Burte, and S. B. Manohar, Phys. Rev. C **53**, 796 (1996).
[26] J. V. Kratz, J. O. Liljenzin, A. E. Norris, and G. T. Seaborg, Phys. Rev. C **13**, 2347 (1976).
[27] D. J. Hinde, M. Dasgupta, J. R. Leigh, J. P. Lestone, J. C. Mein, C. R. Morton, J. O. Newton, and H. Timmers, Phys. Rev. Lett. **74**, 1295 (1995).
[28] P. Mollar and A. J. Sierk, Nature (London) **422**, 485 (2003).
[29] T. K. Ghosh, S. Pal, K. S. Golda, and P. Bhattacharya, Phys. Lett. B **627**, 26 (2005).
[30] C. Rubbia, J. A. Rubio, S. Buono, F. Carminati, N. Fiétier, J. Galvez, C. Gelés, Y. Kadi, R. Klapisch, and P. Mandrillon, Conceptual design of a fast neutron operated high power energy amplifier, CERN Report No. CERN/AT/95-94(ET) (unpublished).
[31] N. G. Puttaswamy, N. M. Badiger, M. Raja Rao, D. K. Avasthi, A. Tripathi, D. Kabiraj, and S. Venkataramanan, in *DAE Symposium on Nuclear Physics*, Bombay, 1991, Vol. 34B (DAE, Mumbai, 1991).
[32] B. P. Ajith Kumar, E. T. Subramaniam, K. Rani, and K. Singh, CANDLE–Collection and Analysis of Nuclear Data using Linux nEtwork, in *DAE Symposium on Nuclear Physics*, Kolkata, 2001 (DAE, Mumbai, 2001).
[33] E. Browne and R. B. Firestone, *Table of Radioactive Isotopes* (Wiley, New York, 1996).
[34] U. Gupta, P. P. Singh, D. P. Singh, M. K. Sharma, A. Yadav, R. Kumar, B. P. Singh, and R. Prasad, Nucl. Phys. A **811**, 77 (2008).
[35] A. Gavron, Phys. Rev. C **21**, 230 (1980).
[36] J. H. Hamilton, A. V. Ramayya, S. J. Zhu, G. M. Ter-Akopian, Yu. Ts. Oganessian, J. D. Cole, J. O. Rasmussen, and M. A. Stoyer, Prog. Nucl. Part. Phys. **35**, 635 (1995); J. H. Hamilton, G. M. Ter-Akopian, Yu. Ts. Oganessian, J. Kormicki, S. J. Zhu, M. G. Wang, Q. Lu, K. Butler-Moore, A. V. Ramayya, W. C. Ma *et al.*, Phys. Rep. **264**, 215 (1996).
[37] G. K. Gubbi, A. Goswami, B. S. Tomar, A. Ramaswami, A. V. R. Reddy, P. P. Burte, S. B. Manohar, and B. John, Phys. Rev. C **59**, 3224 (1999).
[38] A. C. Berriman, D. J. Hinde, M. Dasgupta, C. R. Morton, R. D. Butt, and J. O. Newton, Nature (London) **413**, 144 (2001).
[39] D. J. Hinde, A. C. Berriman, R. D. Butt, M. Dasgupta, I. I. Gontchar, C. R. Morton, A. Mukherjee, and J. O. Newton, J. Nucl. Radiochem. Sci. **3**, 31 (2002).
[40] U. L. Businaro and S. Gallone, Nuovo Cimento **1**, 1277 (1955).
[41] L. M. Pant, R. K. Choudhury, A. Saxena, and D. C. Biswas, Eur. Phys. J. A **11**, 47 (2001).
[42] A. Goswami, A. V. R. Reddy, B. S. Tomar, P. P. Burte, S. B. Manohar, and J. Bency, Radiochim. Acta **62**, 173 (1993).
[43] S. A. Karamyan, F. Narmuratov, and Y. T. Oganessian, Yad. Fiz. **8**, 690 (1968) [Sov. J. Nucl. Phys. **8**, 401 (1969)]; **9**, 715 (1969) [Sov. J. Nucl. Phys. **9**, 414 (1969)]; *Physics and Chemistry of Fission* (IAEA, Vienna, 1969), p. 759.
[44] R. Tripathi, K. Sudarshan, S. Sodaye, B. S. Tomar, G. K. Gubbi, A. Goswami, A. V. R. Reddy, and S. B. Manohar, Radiochim. Acta **90**, 185 (2002).
[45] M. de Saint-Simon, L. Lessard, W. Reisdorf, L. Remsberg, C. Thibault, E. Roeckl, R. Klapisch, I. V. Kuznetsov, Yu. Ts. Oganessian, and Yu. E. Penionshkevitch, Phys. Rev. C **14**, 2185 (1976).
[46] R. Tripathi, K. Sudarshan, A. Goswami, P. K. Pujari, B. S. Tomar, and S. B. Manohar, Phys. Rev. C **69**, 024613 (2004).